The Iraqi Journal For Mechanical And Material Engineering, Vol.21, No1,March. 2021

SHOCKWAVES RESULTING FROM HIGH PRESSURE DIESEL FUEL INJECTION CFD & EXPERIMENTAL GRAPHICAL RESULTS

Ali Hasan
alihasan22@hotmail.com
[1]**Department of Aerospace Engineering, Technical University of Munich, Garching Munich, Germany.**

ABSTRACT

Recent experimental research has shown that when injecting diesel fuel at 5000 bar in a combustion chamber at 300 °K, shockwaves are induced. Such shockwaves have demonstrated their influence on improving combustion, however the mechanism behind this improvement isn't fully understood. This paper takes recently published experimental work another step, using a CFD numerical solution. Graphical results and fluid mechanics theory was then used to explain the impact of such shockwaves on the liquid fuel's droplets thermo fluid effects. Methodology involves building a CFD model capable of handling supersonic and subsonic fluid flows, and then generate graphic results. Graphical CFD results were validated against graphical experimental results, with regards to the presence of shockwaves. Confirming the induction of shockwaves in recent experimental research. It was concluded that shockwaves can influence fuel droplet evaporation rate by influencing; (a) the Nusselt and Prandtl numbers, as shown in Eq. (1) to (4), and subsequently (b) influencing the evaporation of a liquid fuel droplet as in equation (8). Shockwaves are energy carriers and therefor a fuel droplet can be influenced as it is crossed by the shockwave. High pressure fuel injection inducing shockwaves improves air/fuel combustion and not just what is traditional thought (finer droplets & turbulences).

Keywords: Shockwaves, fuel, high pressure injection, CFD, combustion

موجة الصدمة الناتجة عن حقن وقود الديزل عالي الضغط باستخدام ديناميك الموائع الحسابيه والنتائج الرسومية التجريبية

علي محمد حسن

الخلاصة

أظهرت الأبحاث التجريبية الحديثة أنه حينما يحقن وقود الديزل عند 5000 بار في غرفة الاحتراق عند 300 درجة مئوية ، يتم إحداث موجات صدمية. أظهرت مثل هذه الموجات الصدمية تأثيرها على تحسين الاحتراق ، لكن الآلية الكامنة وراء هذا التحسين ليست مفهومة تمامًا. يبني هذا البحث على هذه الاستنتاجات ويقدم تفسيرات حول تاثير الموجات الصدميه باستخدام: نظريات المواءع الحراري, وديناميكيات الموائع الحسابيه. تتضمن المنهجية بناء نموذج قادر على التعامل مع تدفقات السوائل الأسرع من الصوت ودون سرعة الصوت ، ومن ثم توريد نتائج صوريه. تم التحقق من صحة النتائج الرسوميه بالمقارنه مع النتائج التجريبيه, فيما يتعلق بوجود موجات الصدمه. استنتج أن موجات الصدمة يمكن أن تؤثر على معدل تبخر قطرات الوقود من خلال التأثير؛ (أ) أرقام Nusletو Prandtl , كما تبين في المعادلات (1) الى (4) ومن ثم (ب) التأثير على تبخر قطرة وقود سائل كما في المعادلة (8). يعمل حقن الوقود عالي الضغط الذي يسبب موجات الصدمة على تحسين احتراق الهواء / الوقود و ليس فقط كما في المفهوم التقليدي (القطرات الدقيقة والاضطرابات).

Received : 30-9-2020
Accepted :29-12-2020

NOMENCLTURE

u, v, w	Velocities in the x, y, & z directions, (m/s)
C_D	drag coefficient
Nu	Nusselt number for the heat transfer between the air gas and liquid fuel droplet
d_p	liquid fuel droplet diameter (mm)
h	heat transfer coefficient ($W/m^2.^oK$)
k	thermal conductivity of air gas ($W/m.^oK$)
Re	Reynolds number
Pr	Prandtl number
ρ	density (kg/m^3)
V_∞ & V_p	are air gas & droplet velocities respectively (m/s)
μ	dynamic viscosity (Pa.s)
C_p	coefficient of heat capacity ($J/kg.^oK$)
Q_L	heat flux acting on the liquid fuel droplet (J/s)
Q_g	gas's heat flux acting on liquid fuel droplet (J/s)
$\dot{m}_F$	liquid fuel vaporization rate in (kg/s)
L_{vap}	liquid fuel latent heat of vaporization (J/kg)
r_d	liquid fuel droplet radius (mm)
λ_g	gas's thermal conductivity (W/m. $°K$)
T_d	liquid fuel droplet temperature (°K)
T∞	gas temperature far away from the liquid fuel droplet (^oK)
ρ_L	liquid fuel density (kg/m^3)
C_{PL}	liquid fuel specific heat at constant pressure ($K/kg.^oK$)
r	ratio of principal specific heat capacities.

INTRODUCTION

Published experimental work Vera-Tudela W. et al., (2020), involving high pressure injection of diesel fuel in a cold flow condition, revealed the presence of shockwaves. It is believed that such shockwaves can play a role in improving the air/fuel mixing and hence improving combustion. The reason for cold flow analysis is that, typically in a reciprocating engine, diesel fuel enters the combustion chamber as a cold flow. Then the air/fuel mixing gets compressed and ignites once the ignition temperature is reached. What is interesting in the presence of the induced shockwaves, is this, it was previously believed that high fuel pressure injection using a suitable fuel injector produces a finer spray (finer droplets). This creates a better air/fuel mixture and therefore better combustion. However, it turned out not just that, but the induction of shockwaves caused by high pressure 5000 bar fuel injection. Shockwaves play an additional role in improving the air/fuel mixture, see Figure(1). Where the relationship between the fluid's pressure and density properties change due to the elastic

properties of the fluids. This additional role will be scrutinized in this paper, and discussed in details.

METHOD

Capturing shockwaves requires careful and specific CFD settings. Any setting does not mentioned below can be assumed as default settings.

- ANSYS CFX ANSYS CFX, (2020) was used.
- The model was generated as shown in Figure(2a) angled 3D and Figure(2b), zoomed on injector fuel inlet. Then imported into the meshing module. Model is to scale and dimensions can be picked up from the shown scale.
- Since supersonic and subsonic flows are involved, careful meshing is important. Mesh skewness was checked, and was found to be less than 0.9. From the mesh software module, the selected Mesh Metric> giving skewness values; Min 5.84e-8, Max 0.95, Average 0.22, & Standard deviation 0.12. Number of elements used 236,520. For cross grid independence checks, no significant changes were observed with an increase in mesh elements. Therefore continued with the mentioned number of elements. In general the following guides were considered Lee H. H., (2019); (a) Avoid using lower-order tetrahedra/triangles. (b) Higher-order tetrahedra/triangles can be as suitable as other elements provided the mesh is adequately fine. In a coarse mesh condition however, their performance is inadequate and using them is inadvisable. (c) Lower-order prisms are inadvisable. (d) Lower-order hexahedra/quadrilaterals can be used, however their efficiency isn't as good as their higher-order equivalents. (e) Higher-order hexahedra, prisms, and quadrilaterals are the most efficient of all the elements. Hence it is advisable to utilize these elements whenever possible. Where this isn't possible then aim for the higher-order hexahedra-dominant or quadrilateral-dominant mesh. (f) Avoid highly skewed elements and keep angles between 40 & 140. Maximum skewness must be less than 0.95, while the average is less than 0.33. The aspect ratio needs to be less than 5, but can be up to 10 inside the boundary layer Anderson B. et al., (2012).
- Fluid Domain settings; Select ideal gas for the chamber area shown in Figure(2). This will take care of air compressibility effects, since sub-sonic as well as subsonic air flows are considered. In the Fluid Model tab, select Total Energy. Allowing for modelling the transport of enthalpy and kinetic energy effects. This is important where gas dynamics are in the subsonic/supersonic zones. This again is important since the research is aimed at compressibility effects and searching for shockwaves. Viscose effects are also considered, therefore the viscous term is activated. Select the Reynolds Stress Model SSG. The advantages in this selection are; (a) suitable for complex flows where the turbulent-viscosity models can be unsuccessful, (b) considers anisotropy (unequal physical properties along different axis).This is important, since the high pressure droplets dispersion flows are expected to move in various directions with shockwave effects, & (c) Performs well with complex flow patterns; flow separation, swirl, and planar jets. While the disadvantages are; (a) it's 11 transport equations makes it computationally expensive, (b) the transport equations have several terms which need to be closed (c) because of the so many introduced closures in the model, performance can be poor for some flows Anderson B. et al., (2012). This selection of the SSG turbulence model will need to monitored per a specific case, for performance, it is relatively new compared to the well-established turbulence models such as the; k-ε & k-ω models. Regarding the fuel selection, create a fluid name spray in the Fluid and Particle Definitions. Assign the material $C_{10}H_{22}$ as diesel, imported from the materials built in data library. Select

Martial>Morphology>Option>Dispersed Fluid, and a Mean Diameter 0.5 micron. Select Volume Fraction as 1. In the Fluid Pair Models select 28e-3 N/m for surface tension between air & fuel. For Momentum Transfer>Drag Force>Option>Schiller Naumann. Heat Transfer>Option>Ranz Marshall. The Fluid Domain reference pressure was set at 1 atm, while the temperature was assumed to be 300 ºK. Noting, that in the referenced experimental work Vera-Tudela W. et al., (2020), the chamber's temperature was 650 °K. This was deliberately set differently at 300 °K, to demonstrate that shockwaves can happen and not solely dependent on temperature.

- For Boundary Conditions. Select for the Fuel injection inlet; Flow Regime>Option>Mixed. Since it is expected to have both supersonic and subsonic flows. Select Blend Mach No. Type>Normal Speed, Option>Cart. Vel. & Total Pressure> Rel. Total Pressure 5000 bar, u, v, w at 200, 200 & 200 m/s respectively. Turbulence>Option>High Intensity 10%. Static Temperature 300 °K. In the Fluid Values tab, select for Volume Fractions; 0 for air, and 1 for fuel spray inlet. Fuel injector type used in the experiment is shown in the top right corner of Figure(1), fuel inlet 190 micron.
- Solver Settings Al Makky A. (2018) specifics are; (a) Basic Settings>Advection Scheme>Option>Upwind. (b) Transient Scheme>Option>first Order Backward Euler. (c) Turbulence Numerics>First Order. (d) Residual Target 1e-4. (e) Time Control> Physical Timescale>1e-12 s, an extremely small value chosen to allow for picking-up supersonic/subsonic shockwaves. Also important that the time step size should be sufficient in representing a fluid particle crossing a cell. Naturally the smaller the time step is, the longer time it takes to complete processing. Therefore, the time step needs to be kept just sufficient for the fluid particle to cross a cell. (f) In the Advanced Options tab, select; Interpolation Scheme>Pressure Interpolation Type>Trilinear. (g) Select; Velocity Interpolation Type>Trilinear. (h) Select; Compressibility Control. (i) Select; High Speed Numeric. Selections are made on the basis of the above mentioned reference, and personal experience as will be demonstrated in the Results and Discussions section. Since the Residual Target is set, the processor will continue to run until the set targets are reached. Note the timescale is extremely small, and this can take some time, depending on computing resources used.
- Schiller Naumann empirical equation, equation (1), is used for drag coefficient C_D prediction in the present work. This equation is developed for laminar flow.

$$C_D = 24(1 + 0.15Re^{0.687})/Re \text{ where } Re \leq 1000, \text{ and } C_D = 0.44 \text{ where } Re > 1000 \quad (1)$$

More accurate equations are available capable of handling turbulent flows such Baker and Land models Karimi M. et al., (2012). A short discussion in Appendix 1 is also given, with regards to peak C_D values, M number and Re number. Hence showing the difference between equation (1) with the assumption of a constant C_D value for Re > 1000, and how C_D values vary with flow Mach number, see Appendix 1.

- Ranz Marshall correlation, equation (2), covers the heat transfer between the spherical droplet and the surrounding air gas media is used in the present work. This is added to cater for any heat transfer that may exist between the liquid droplet and air. Though could be insignificant since the supersonic or subsonic, nevertheless is considered for accuracy.

$$Nu = h.(d_p/k) = a + cRe^m.Pr^n \quad (2)$$

Where a, c, m, & n are numerical constants determined by the considered fluid and flow geometry AISSA A. et al., (2013). A quick inspection of Equations (1) & (2) shows for an

instance the impact of shockwave (velocity changes) on the Re number, and hence the fuel drag force and the droplet Nu number. One example of shockwaves influencing the fuel droplets drag forces and rate of evaporation. There are various Nu empirical correlations developed. Such as: -

Lewis & Marshall Lewis A., et al., (1973), Ettouil B.F. et al (2008)
Fiszdon Ettouil B.F. et al (2008), Young R. M., et al (1985)
Lee & Pfender Young R. M., et al (1985)
Kalganova Lewis A., et al., (1973)

All equations are influenced in the same was as Ranz & Marshall. However, focusing on the subject of discussion, the same influences covered in this paper apply to these equations.

- Upwind is a first order scheme, more robust than the second order High Resolution scheme. It also depends on the upstream conditions, in this case the injector inlet, and generally converges better.
- First Order Backward Euler is one of the most basic numerical method for the solution of ordinary differential equations. The backward Euler method has error of the order one in time. It's an implicit method (unlike the Forward Euler which is explicit) known to be computationally expensive but stable Backward Euler method, (2020), Zeltkevic M. (1998). It is selected due to its stability in resolving mixed supersonic/subsonic flows.
- Trilinear preferred over linear. Suitable where a large number of 3D grids look-ups are required.

RESULTS AND DISCUSSIONS

Results revealed shockwaves induced by the sudden changes in high pressure flow. The beta variable in ANSYS CFX software is offered in the high resolution differencing scheme, capable of minimizing velocity under & over shoots. See Figure(3), for results, fuel spray velocity (u) .Beta.Gradient. CFD Settings showed how sound selections based on similar published work can pick up shockwaves. Validating Figure(1), v Figure(2), shockwaves are visible and in the form of bands. Figure(3), identified changes in velocity (velocity gradients), velocity influences the Re number, as in Equation(3). In both images the fluid volume showed larger shockwave rings in almost the middle volume portion, see the blue vertical arrows. The results demonstrate what can happen at the point of diesel fuel injection, where air has just filled the cylinder and fuel injected at 5000 bar in a cold flow. Naturally what actually happens is once the fuel mixture is injected it gets compressed with air, and heats up. Timing issues make a difference; however, the object of this paper is to demonstrate what happens at a specific instance in time. That is as the fuel is injected, shockwaves play a role in breaking up the fluid volume in two larger portions, two in this example. Also in between the shockwaves smaller volume portions exist, this can be seen in Figures (1, 2 & 3). A possible explanation can be referenced to Equation (1), as Re increases, so does C_D. Till the point is reached where C_D increases so much, then begins to separate, at the shock waves locations. What is also shown in the experimental and CFD images is the existence of smaller shockwaves which again though smaller in magnitude, but do contribute to air/fuel mixing. Noting that the above is a steady state CFD numerical solution, a transient solution can show more. However computing resources have limited the scope of work to a steady state, transient simulation with extremely small time step, necessary to capture supersonic/subsonic flows is computationally expensive. More in depth discussions on how Equations (1) & (2) are effected, reveal how the issue is complex. Thermofluids properties are interconnected, examples.

$$\mathrm{Re} = \frac{\rho_\infty (V_\infty - V_p) d_p}{\mu} \quad (3)$$

$$\mathrm{Pr} = \frac{\mu C_p}{{}^\circ K} \quad (4)$$

Shockwaves will influence all above parameters, example Equation(3); density is influenced by shockwaves influencing air density (changing compression/pressure), Figure(4). Velocity levels influenced as shown in Figure(3), and d_p is influenced by changes reflected in Equation (2). In Equation (4); dynamic viscosity is influenced by temperature example 1e-3 Pas a 40 °C, & 3e-3 Pas at 0 °C Massey B., et al (2006), C_p & K are influenced by the amount of heat received and linked with the Nu value in Equation (2), hence shockwave velocity. Proving through established equations that such shockwave influences the fuel droplet vaporization. Thus, not just purely increased turbulences providing a better contact between air molecules and fuel droplets. Such a development can certainly benefit the piston engine of all fuel types and not just diesel engines. Including other form of combustion, can utilize such information. No doubt any changes in temperature and pressure will impact shockwaves, since air density will change. A closer look at a liquid fuel droplet vaporization mechanism, shows how shockwaves are linked to this phase change. Equation (5) explains the link between vaporizing rate and heat, based on the individual Equation (6) to (8). The assumption used to develop these equations is that the evaporating droplet is axisymmetric. Equation (6) shows how Qg is influenced by Nu, where Nu in turn is influenced by Re, see Equation. (2). Figure (5), illustrates the thermodynamics of a fuel droplet going through a phase change, liquid to vapor. Shockwaves and the induced velocity effects impact the Re number, subsequently impacting the Nusselt number. Heat flux entering droplet Crowe C. et al. (1998);

$$Q_L = Q_g - \dot{m}_F L_{vap} \quad (5)$$

Heat flux from the gas to the droplet body Sirignano W. A., et al (2010);

$$Q_g = 2\pi r_d \lambda_g N_u (T_\infty - T_d) \quad (6)$$

The following differential equations (Crowe C. et al. 1998) calculates the evolution time for the droplet's r_d at a temperature T_d.

$$Q_L = \frac{4}{3}\pi r_d^3 \rho_L C_{pL} \frac{dT_d}{dt} \quad (7)$$

$$-\dot{m}_F = 4\pi r_d^2 \rho_L \frac{dr_d}{dt} \quad (8)$$

Shockwave behavior and possible impacts on a fuel droplet are discussed in this paragraph. Shockwaves are either oblique or normal. Oblique are not perpendicular to the direction of flow, which is not the case as shown in Figure(1). The normal shockwave fits the pattern shown in Figure(1), and shockwaves occur in the air media downstream of the fuel spray. This can be explained due to the sudden release of high pressure liquid fuel spray, and subsequently pushing the air molecules, causing ripple effects. Air as is compressible gas with its elastic properties, acts like a spring reacting in the form of waves. It is known that shockwaves occurring in the direction of flow are supersonic, while that downstream is subsonic and at a higher pressure. Changes occurring in a shockwave are irreversible, hence not isentropic. Equation 9 is the Rankine - Hugoniot relation Massey B., et al (2006) shows the relationship of pressure and density before and after the shockwave, see Figure(7). Indicating that the changes in a shockwave are irreversible, and therefore not isentropic. Since it isn't the same as p/ρ^γ = constant, a reversible adiabatic process. The higher the ratio of p2/p1, the more Equation(9) diverges from the isentropic air, $\gamma = 1.4$. Shockwaves is a specialized area of knowledge, and therefore its theoretical discussions are kept to the point.

Depicting the evidence of the shockwave's influence on a liquid fuel droplet. Influencing Equation (1) to (8) with; pressure, density, velocity, and temperature. Which means a fuel droplet phase change effects does depend on its location with regard the shockwave, as in Figure(7). Meaning, a fuel droplet at the location shown Figure(6), will experience the physical parameters shown to the left. Whereas if it was across the other side of the shockwave physical parameters to the right are applicable

$$\frac{\rho 2}{\rho 1} = \frac{\gamma - 1 + (\gamma + 1)P2/P1}{\gamma + 1 + (\gamma - 1)P2/P1} \quad (9)$$

$$T2/T1 = (p2.M2/p1.M1)^2 \quad (10)$$

Wrapping up the impact of a shockwave; a shockwave is a propagating fluid disturbance moving faster than the surrounding speed of sound, a shockwave carries energy, propagates through a medium but characterized by an abrupt, almost discontinuous, change in the medium temperature density & pressure, as in Figure(6).

CONCLUSIONS AND OUTLOOK

Experimental and CFD numerical results have demonstrated the influences of shockwaves caused by high pressure diesel fuel injection. Diesel fuel injected at 5000 bar, improves air/fuel mixing conditions due to; (a) Increased finer droplets and turbulences, which is an already established fact. (b) Shockwaves influencing the fuel's droplet evaporation rate, demonstrated through Equations (1) to (8). (c) Specific links were drawn between the role of Nu on a fuel's droplet vaporizing rate and the Re number. Where the Re number is dependent on the air flow velocity, and this velocity is influenced by changing velocity gradients. (d) Shockwaves are energy carriers with thermofluid properties capable of influencing a liquid fuel droplet. Demonstrated through Figure(6), Equations (9) & (10). (e) Shockwaves can influence rate of fuel droplet vaporization as proven in (c) and therefore as a result, improve fuel combustion. The CFD numerical solution with suitable supersonic/subsonic performed exceptionally well in picking up shockwaves. Graphical results validated in Figures (1) and (2), showing shockwaves almost half way across the chamber length. The Reynolds Stress Model SSG performed exceptionally well, confirming its suitability for complex flows. However, it was found computationally expensive as it is known to be. It was necessary to use an extremely small Physical Timescale of 1e-12 s, to reach convergence. The outlook is to continue with this kind of research with different; fuels, chamber dimensions, and chamber fluid temperature. Based on current findings maximum C_D values for spherical bodies occurs between Mach 1.5 & 2, as indicated in Appendix 1. This needs to be further researched, as it may show that there is an optimal high pressure for optimal liquid droplet vaporizing. Higher injection pressures beyond a certain level could prove to be counterproductive, higher equipment costs with insignificant gains. Since the C_D value at higher M values can cause a drop in Re value (see in appendix 1), subsequently lowering the N_u value (in equation 2), and eventually lowering the heat flux to the droplet Q_g in equation (6).

ACKNOWLEDGEMENTS

Thanks to Mr Abdulkadir Benzamia and Abdulafoo Parkar of Flowpak WLL, Qatar for their recommendations on best CFD meshing practices. Thanks to Dr W. Vera-Tudela, Department of Mechanical Engineering, ETH Zurich, Switzerland. For allowing the referencing in this paper the; experimental data findings on shockwave effects on fuel spray droplets and related images.

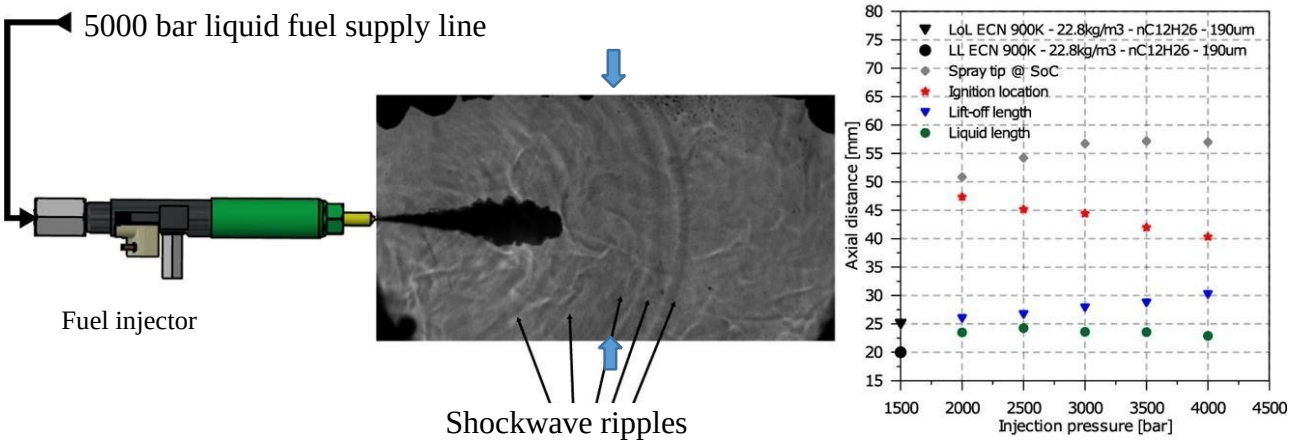

Fig. (1): Shockwaves high speed photography showing shockwaves. Image supplied curtsey of (VeraTudela W. et al., 2020).

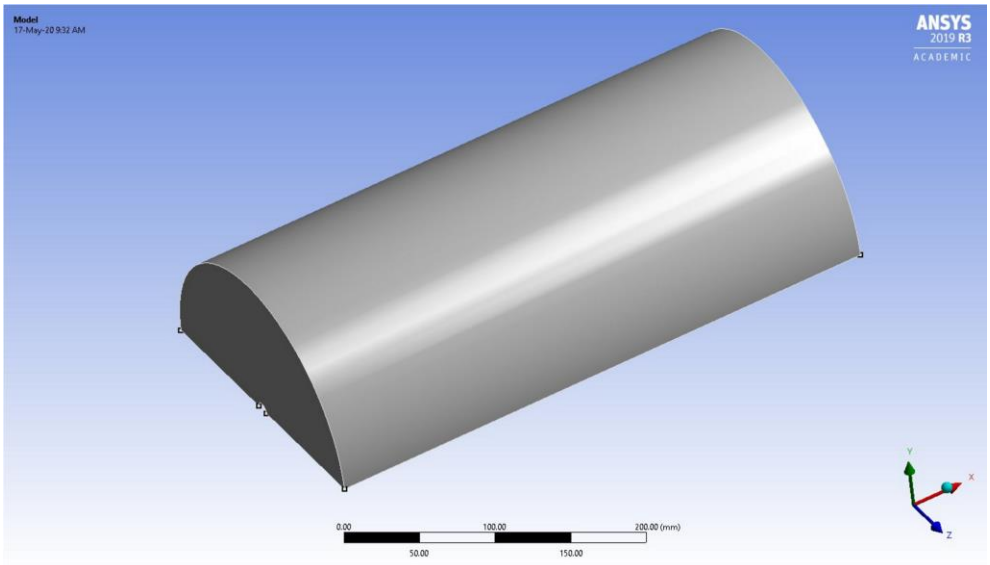

(a): injector inlet shown to the left.

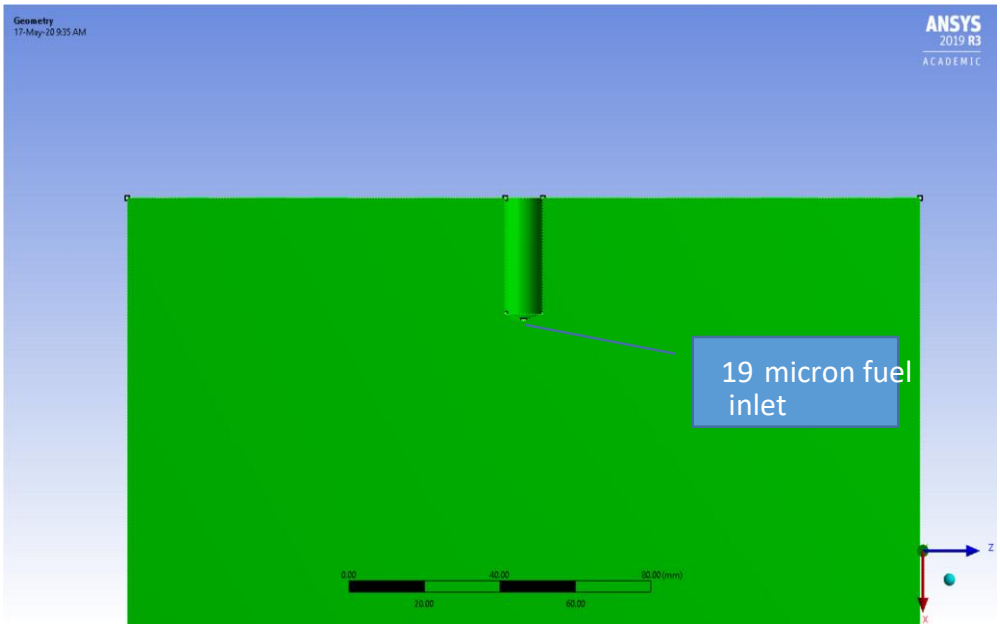

(b) Injector location showing fuel inlet details.

Fig.(2) Angled 3D image, for fuel chamber

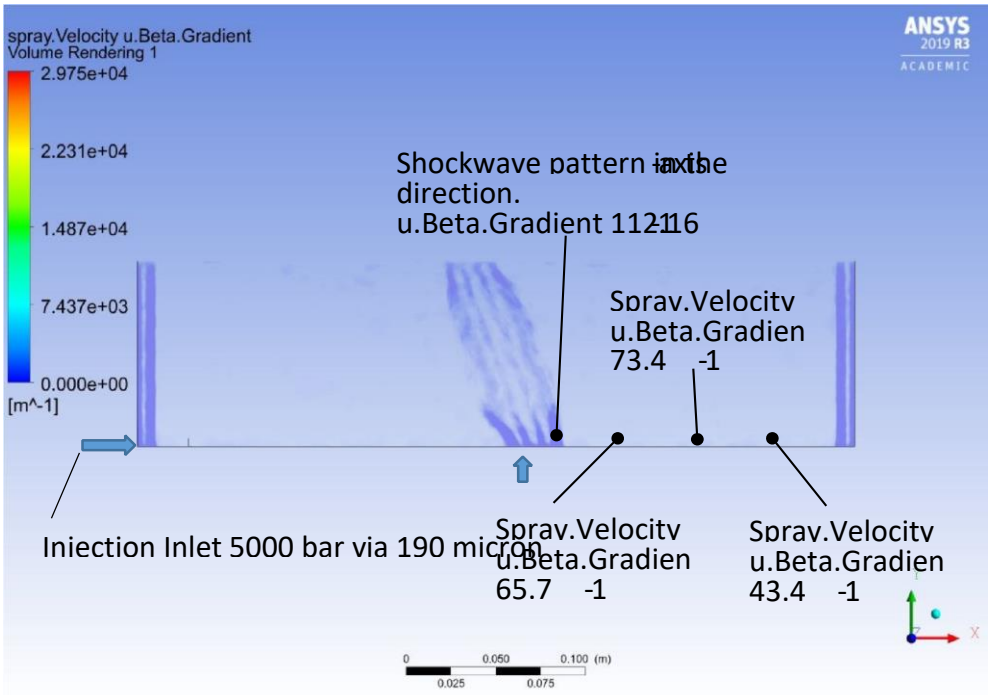

Fig. (3): Shows a pattern of shockwaves, non-uniform velocity flow. A pattern of high velocity gradients and a pattern of smaller scale of velocity gradients

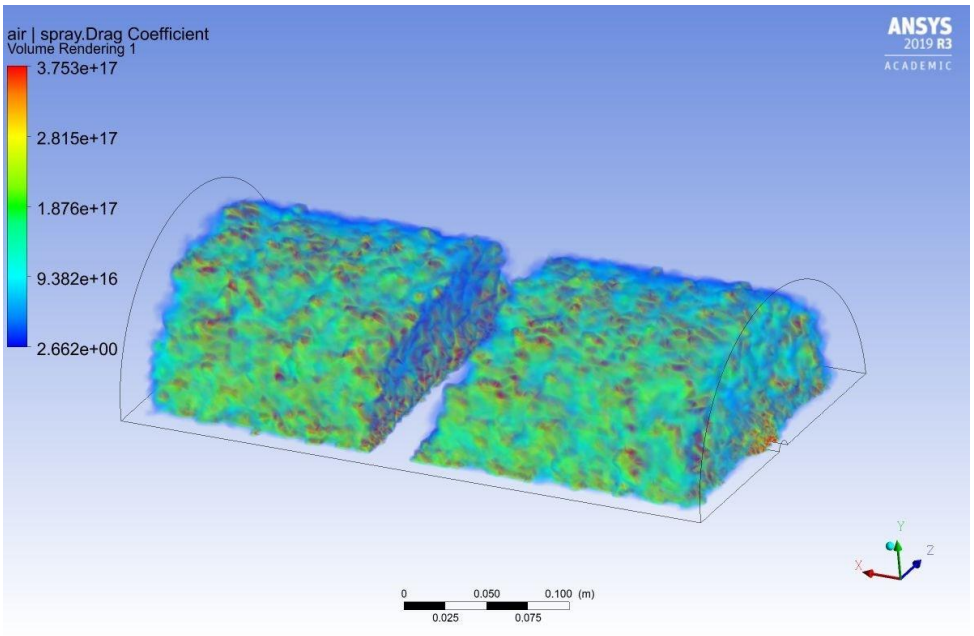

Fig. (4): Demonstrating the impact of the shockwaves on fluid flow dynamics. Almost separated the fluid volume flow into two halves.

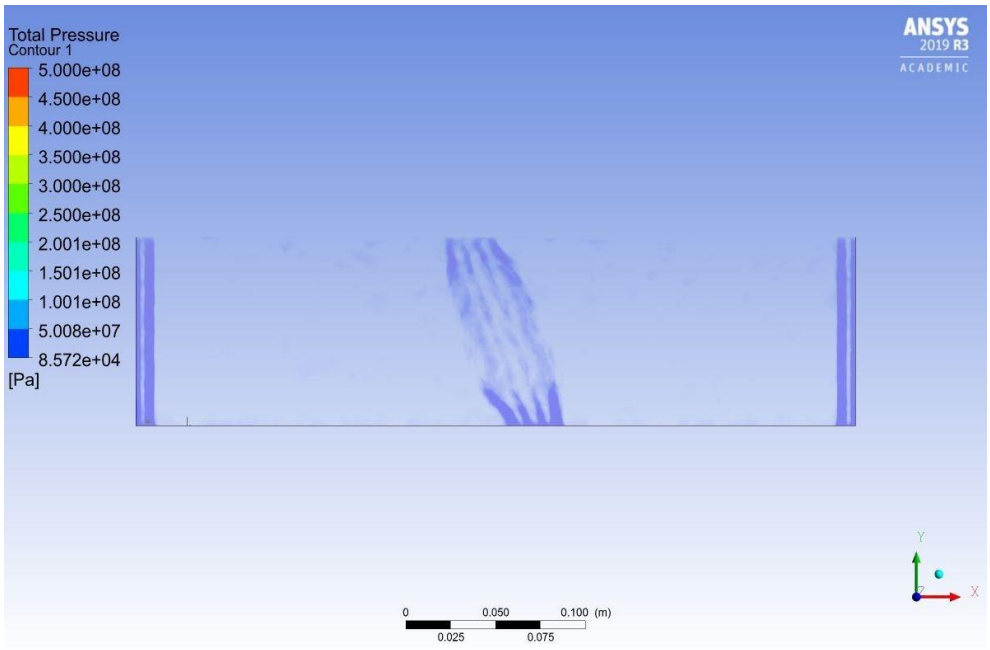

Fig. (5): Shockwaves influencing pressure waves.

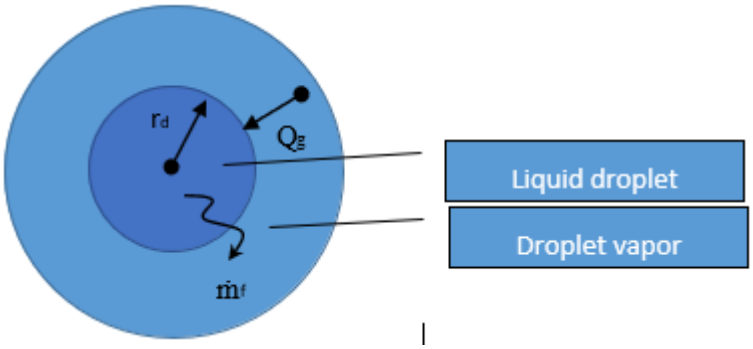

Fig. (6): Example showing a liquid phase droplet surrounded by its vapor phase product.

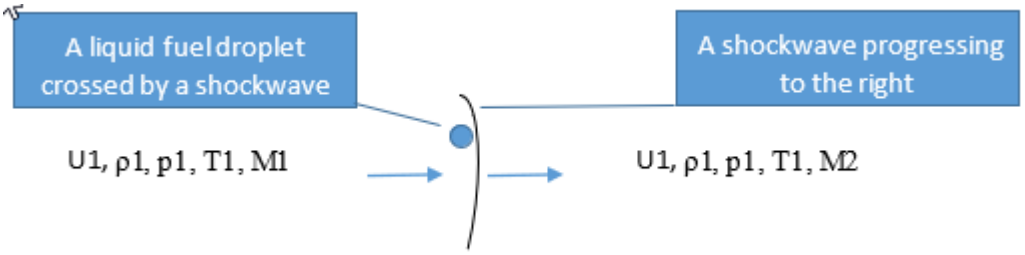

Fig. (7): Gas properties downstream and upstream of a

APPENDIX 1

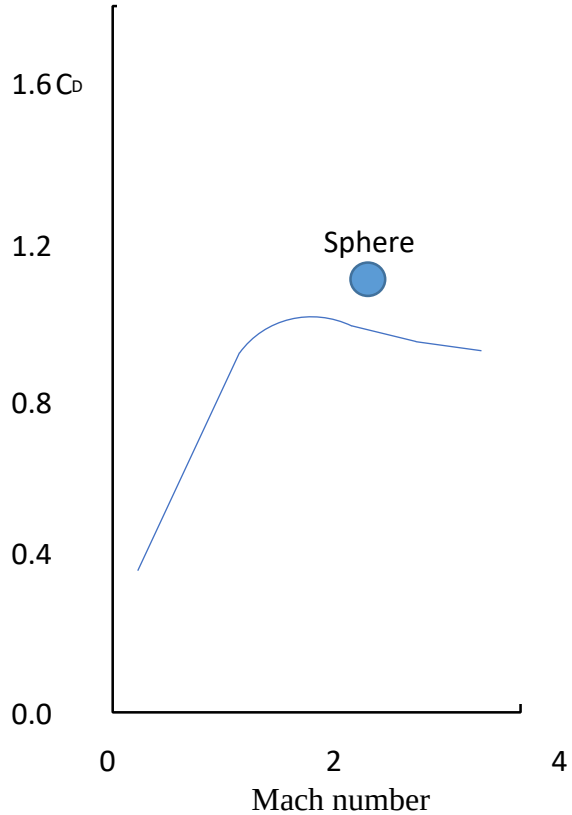

C_D values change with Mach number, and therefore the so does the Re number as in equation (3).

Highlighting the differences between equation (1) assumptions of a constant C_D = 0.44 @ Re > 1000 and how the C_D value actually varies with the Mach number (higher Re numbers).

Fig. (8): Coefficient of Drag C_D vs. Mach number (M), a relationship between fluid flows over a specific body shape. A sphere representing a liquid droplet in this case.

Figure (8) indicates how the C_D value varies against the M number for a specific body shape. A liquid fuel droplet in this case (Massey B., et al 2006). The Relationship of C_D and the Re number which in turn is influenced by the M number, is captured in equation 1. Another words the fuel droplet's shape does influence the Re number, and hence all the equations referred to in this paper which depend on the Re number. Example equation (2) has shown how the Re number influences the N_u number, and subsequently the Nu number influencing Q_g in equation (6). A closer look on Figure(7) shows how the wave drag intensifies as the M number increases, summiting between 1.5 & 2.0 M. Then beyond approximately 2.0 M C_D decreases towards an asymptotic value. A quick inspection of equation (1) shows; by substituting Re 600 & then 1000, the C_D values are 0.52 & 0.44 respectively. Schiller Naumann 's equation assumes CD = 0.44 constant for all Re values above 1000. The following plot represents equation (1), plot generated electronically, using online software (Math Power, 2020). The Re & CD numbers are always positive, therefore just consider the top right quarter of Fig. 8 (a).

NOTE: Figure (8) is illustrative only. Physically the C_D values are never this high, see Figure(7) for C_D values.

Figure 9 (b) shows higher Re numbers, see section 2 & equation (1) discussions. Low Re numbers were considered, Re ≤ 1000, since this equation was based on laminar flow.

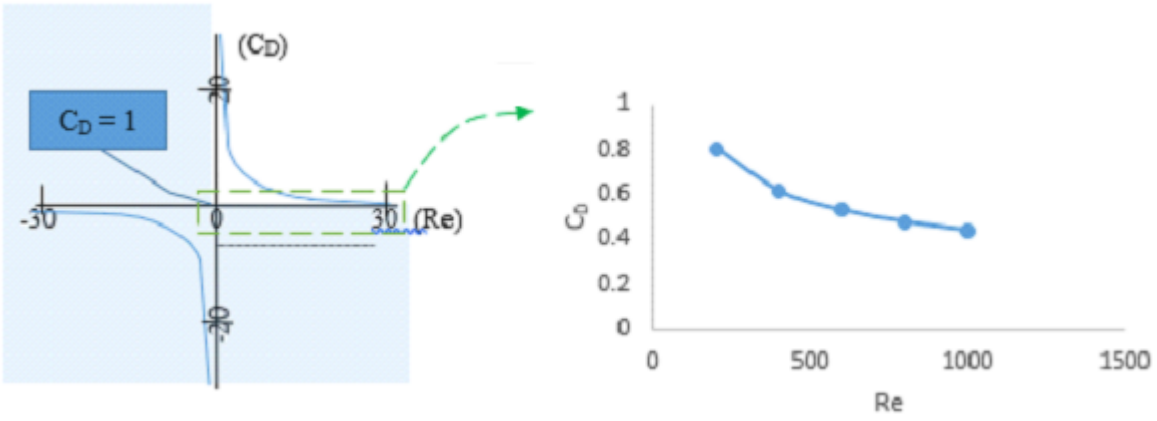

(a) (b)

Figure (9): An indicative plot of C_D v Re number based on equation (1) - Schiller Naumann equation. (a) A general plot with a Re number up to 30. (b) Higher Re numbers with a C_D number up to 1.

REFERENCES

A Al Makky.. Shock Waves Simulation. http://cfd2012.com/ansys-cfx-compressible-flows.html, 2018.

ANSYS CFX. ANSYS Academic software version, ANSYS Inc (2020). USA.

Anderson B., Andersson R., Hakansson L., Mortensen M., Studiyo S., & van Wachem B. . Computational Fluid Dynamics for Engineers. Cambridge University Press. P 175 & 100. ISBN 978-1107-01895-2, 2012.

Aissa a., Abdelouahab m., Noureddine a., Elganaoui m., Pateyron b. . Ranz & Marshall, Correlations limits on heat flow between a sphere and its surrounding gas at high temperature", Laboratoire de Modélisation & Optimisation des Systèmes Industriels, Université des Sciences et de la Technologie - Mohammed Boudiaf - BP 1505 - Oran – Algérie. P 2, 2013.

Backward Euler method. Wikipedia. http://en.m.wikipedia.org/wiki/Backward_Euler_mthod, 2020.

Crowe C. et al. Multiphase flows with droplets and particles, CRC Press LLC. ISBN 0-8493-9469-4, 1998.

Ettouil B.F., Mazhorova O., Pateyron B., Ageorges H., El Ganaoui M., & Fauchais P." Predicting dynamic and thermal histories of agglomerated particles injected within a d.c. plasma jet", Surface and Coatings Technology journal, 202, pp. 4491-4495, 2008.

Karimi M., Akdogan G., Dellimore K. H., & Bradshaw S. M. . Comparison of different drag coefficient correlations in the cfd modelling of a laboratory-scale rushton-turbine flotation tank". Ninth International Conference on CFD in the Minerals and Process Industries CSIRO (2012), Melbourne. P 2, Australia 10-12 December 2012.

Lee H. H., Finite Element Simulations with ANSYS Workbench 2019 Theory, Applications, Case Studies. P 13. ISBN: 978-1-63057-299-0, 2019.

Lewis A., & Gauvin W.H.. Motion of particles entrained in a plasma jet, Aiche Journal, 19, pp. 982– 990, 1973.

Math Power. Mathpower.com. https://www.mathepower.com/nullstellen.php, 2020.

Massey B., & Ward-Smith J. . Mechanics of Fluids 8th edition. Taylor Francis London & New York. ISBN 0-203-41352-0. P 668, 500 & 341, 2006.

Sirignano W. A. Fluid dynamics and transport of droplets and sprays - Second edition, Cambridge University Press. ISBN 978-0-521-88489-1, 2010.

Vera-Tudela W. et al. An experimental study of a very high-pressure diesel injector (up to 5000 bar) by means of optical diagnosis, Fuel 275 117933, 2020.

Young R. M., & Pfender E.. Nusselt Number Correlations for Heat Transfer to Small Spheres in Thermal Plasma Flows. Plasma Chemistry and Plasma Processing, Vol. 7, 1985.

Zeltkevic M., Forward and Backward Euler Methods. http://web.mit.edu/10.001/Web/course_Notes/Differential_Equations_Notes/node3.html, 1998.